

- (Plenum, New York, 1987), pp. 415–427.
4. M. Filion, L. Tremblay, P. J. Bédard, *Brain Res.* **444**, 165 (1988).
 5. H. Bergman, T. Wichmann, M. R. DeLong, unpublished data.
 6. Surgical procedures were performed under pentobarbital anesthesia (Sodium Pentobarbital, Butler, OH; 35 mg per kilogram of body weight); MPTP (MPTP hydrochloride, Aldrich, Milwaukee, WI; 0.4 mg/kg per day, intramuscularly) was given for a total of 10 days (monkey C-67) or 15 days (monkey D-32). IBO (Regis, Morton Grove, IL; 10 µg/µl in phosphate-buffered saline) was applied as bolus injections (0.2 µl every minute; a total of 2 µl at one location in monkey D-32 and a total of 7 µl at four different locations in monkey C-67).
 7. The behavior of the monkeys in their home cages was videotaped and the monkeys were neurologically examined. A computer-assisted method of behavioral assessment was used to quantify the amount of tremor and movement. An observer watched the monkeys in their home cages and pressed specific keys on a keyboard whenever movement or tremor occurred. The computer measured the amount of time given keys were pressed. This method was used during the MPTP- and IBO-treated stage in monkey C-67 and throughout all stages of the experiment in monkey D-32. An accelerometer (Entran Devices, Fairfield, NJ) attached to the wrists or heads of the monkeys was used to obtain power spectra of tremor. The output was amplified, filtered (0 to 50 Hz), digitally sampled at 200 Hz, and processed off-line. The forearm displacement evoked by application of elbow torque pulses yielded a measure of rigidity. For this, the monkeys were seated in a primate chair with one arm in a manipulandum through which flexion torque pulses (60 ms; 0.1 N-m), generated by a torque motor, were applied. The manipulandum was coupled to a potentiometer with an output, indicating the position of the handle, that was digitally sampled at 100 Hz and averaged over 5 to 15 trials to calculate maximal displacement values.
 8. R. Hassler, T. Reichert, F. Mundinger, W. Umbach, J. A. Gangleberger, *Brain* **83**, 337 (1960).
 9. H. Narabayashi, in *Stereotaxy of the Human Brain*, G. Schaltenbrand and A. E. Walker, Eds. (Thieme, Stuttgart, 1982), pp. 510–514.
 10. Y. Lamarre and A. J. Joffroy, *Adv. Neurol.* **24**, 109 (1979).
 11. E. Svennilson, A. Torvik, R. Lowe, L. Leksell, *Acta Psychiatr. Neurol. Scand.* **35**, 358 (1960); L. V. Laitinen and M. I. Hariz, *Movement Disorders* **5**, suppl. 1, 82 (1990).
 12. J. R. Whittier and F. A. Mettler, *J. Comp. Neurol.* **90**, 319 (1949); C. Hammond, J. Feger, B. Bioulac, J. P. Souteyrand, *Brain Res.* **171**, 577 (1979); A. R. Crossman, M. A. Sambrook, A. Jackson, *Brain* **107**, 579 (1984); I. Hamada and M. R. DeLong, *Soc. Neurosci. Abstr.* **14**, 719 (1988).
 13. J. P. Martin and N. S. Alcock, *Brain* **57**, 504 (1934); R. B. Dewey and J. Jankovic, *Arch. Neurol.* **46**, 862 (1989).
 14. T. Klockgether and L. Turski, *Trends Neurosci.* **12**, 285 (1989).
 15. We thank A. P. Georgopoulos and G. E. Alexander for reading the manuscript, C. A. Kitt for assistance with the histology, G. L. Wenk for help with IBO, and L. H. Rowland for technical assistance. Supported by NIH grant 5 R01 NS15417-09 and by a gift from the E. K. Dunn family. H.B. was a Chaim Weizman fellow.

29 March 1990; accepted 2 July 1990

between these two genes) (2, 6). The third feature is within the intracellular domain and consists of six *cdc10/SWI6* repeats, a motif shared by molecules associated with cell-cycle regulation in yeast (*cdc10*, *SWI4*, and *SWI6*), human erythrocyte ankyrin, a sex-determining gene in *C. elegans* (*fem-1*), and a human proto-oncogene (*bcl-3*) (8). *Xotch*, like *Notch*, has exactly 36 EGF-like repeats. If the regions containing the EGF-like repeats in *Notch* and *Xotch* are aligned, 51% of the amino acids are identical. A similar alignment of *Xotch* to either *lin-12* or *glp-1* produces a lower match (36% and 39%, respectively) (5–7). Closer analysis of individual repeats shows that *Xotch* and *Notch* share amino acids in addition to the ones that make up the consensus sequence and that even irregular spacings are preserved between corresponding repeats. This conservation implies that the repeats are not interchangeable and that minor differences between each repeat are required for function. Such an interpretation is supported by genetic analysis of *Drosophila Notch* in which a single amino acid change within the repeat region can result in a mutant phenotype (9, 10). The portion of *Xotch* most highly conserved relative to *Notch* (70% identity) contains the cytoplasmic *cdc10/SWI6* repeats and downstream 30 amino acids. This degree of conservation further indicates the probable involvement of this region in mediating the intracellular functions of the *Xotch* and *Notch* proteins (8).

Some areas of similarity between *Notch* and *Xotch* are not shared by *lin-12* and *glp-1*. One area is a stretch of polyglutamine residues encoded by a sequence referred to in *Drosophila* as the *opa* or M-repeat (11). The *opa* repeat has no known function, but is a molecular feature found in many *Drosophila* genes. The presence of an apparent skeleton of the *opa* repeat in the *Xotch* sequence is further evidence of the relatedness of these molecules. Another area of similarity, at the extreme COOH-terminus, contains a cluster of proline, serine, and threonine residues referred to as a PEST sequence, some of which are putative sites of phosphorylation (12, 13). The PEST sequence may be involved in decreasing protein stability. The similarities between *Xotch* and *Notch* indicate that the two are homologs and suggest that both could have identical functions during development.

To analyze the functions of *Xotch*, we began by studying the expression of *Xotch* RNA during frog embryogenesis using a ribonuclease (RNase) protection assay (14). The pattern of *Xotch* expression was similar in many respects to the pattern of *Notch* expression that has been described for fly development (9, 15). *Xotch* RNA was pre-

Xotch, the *Xenopus* Homolog of *Drosophila Notch*

CLARK COFFMAN, WILLIAM HARRIS, CHRIS KINTNER

During the development of a vertebrate embryo, cell fate is determined by inductive signals passing between neighboring tissues. Such determinative interactions have been difficult to characterize fully without knowledge of the molecular mechanisms involved. Mutations of *Drosophila* and the nematode *Caenorhabditis elegans* have been isolated that define a family of related gene products involved in similar types of cellular inductions. One of these genes, the *Notch* gene from *Drosophila*, is involved with cell fate choices in the neurogenic region of the blastoderm, in the developing nervous system, and in the eye-antennal imaginal disc. Complementary DNA clones were isolated from *Xenopus* embryos with *Notch* DNA in order to investigate whether cell-cell interactions in vertebrate embryos also depend on *Notch*-like molecules. This approach identified a *Xenopus* molecule, *Xotch*, which is remarkably similar to *Drosophila Notch* in both structure and developmental expression.

D*rosophila Notch* IS A GENE REQUIRED for local cell-cell interactions that specify cell fate in the fly embryo (1). Although the mechanisms underlying these interactions are not fully understood, the *Notch* gene product probably functions at the cell surface by permitting determinative interactions between cells. Because similar forms of cell interactions may also occur in vertebrate embryos, we probed

an early neurula *Xenopus* cDNA library with *Notch* DNA using low stringency hybridization (2–4). This screening resulted in two overlapping cDNA clones that correspond to a 10-kb transcript and encode the amino acid sequence of *Xotch* (Fig. 1A). *Xotch* contains the three structural features by which *Notch* and the two nematode genes *lin-12* and *glp-1* are classified as a family of determinative, cell interaction molecules (Fig. 1B) (2, 5–7). Two of these features form a single extracellular domain consisting of multiple epidermal growth factor (EGF)-like repeats (10 to 36) and three *lin-12/Notch* repeats (defined by a region of similarity

C. Coffman and W. Harris, Department of Biology, University of California, La Jolla, CA 92093.
C. Kintner, Molecular Neurobiology Laboratory, The Salk Institute of Biological Studies, P.O. Box 85800, San Diego, CA 92138.

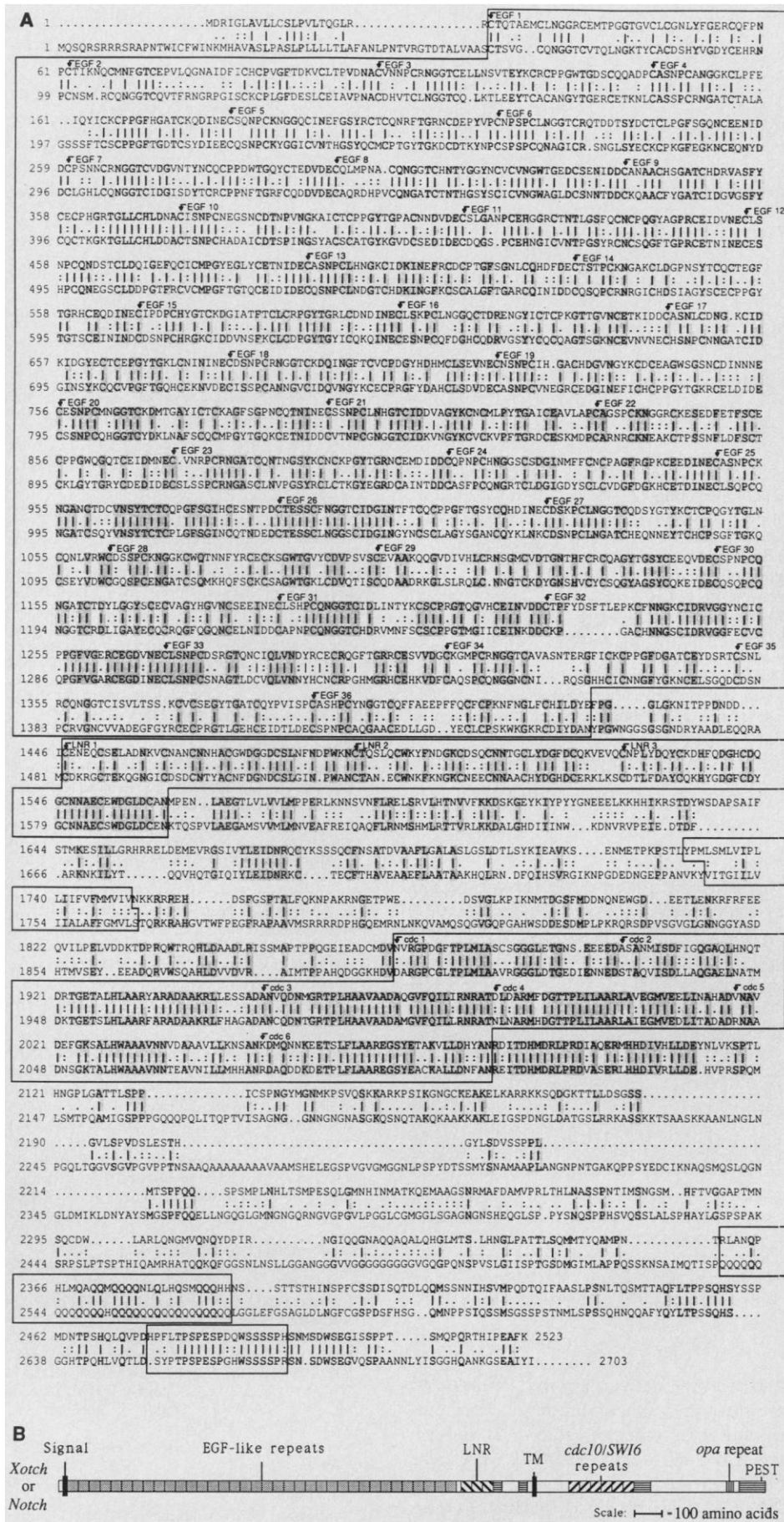


Fig. 1. Alignment of the amino acid sequences of *Xotch* and *Notch*. **(A)** The amino acid sequence (20) of *Xotch* was predicted from the nucleotide sequence of selected cDNA clones and aligned to the published sequence of *Drosophila Notch* (2) with the University of Wisconsin sequence analysis programs (21). The *Xotch* sequence is on the top, *Notch* sequence on the bottom, and identical amino acids are highlighted with a gray box. The outlines mark large regions of sequence that correspond to major structural features of *Xotch*, including the 36 EGF-like repeats (amino acids 22 to 1429), the three *lin-12/Notch* repeats (amino acids 1467 to 1562) (6, 7), a hydrophobic transmembrane domain (amino acids 1728 to 1751), six *cdc10/SWI6* repeats (amino acids 1869 to 2082) (8), the ghost of *opa* repeat (amino acids 2359 to 2391) (11), and the PEST sequence in the COOH-terminus (amino acids 2475 to 2495) (13). Other regions of similarity between *Xotch* and *Notch* are found in the first 30 residues downstream of the *cdc10/SWI6* repeats and in the extreme COOH-terminus of the protein including a number of possible phosphorylation sites (12). **(B)** Schematic representation of the putative *Xotch* or *Notch* proteins. Representation of major features is as follows: hydrophobic signal sequence (solid bar), EGF-like repeats (shaded), *lin-12/Notch* repeats (LNR; right hatches), a single transmembrane domain (TM; second solid bar), *cdc10/SWI6* repeats (left hatches), nonmotif regions of >40% identity between *Xotch* and *Notch* (horizontal lines), *opa* repeat (vertical lines), and a PEST sequence.

sent maternally and the amount per embryo remained relatively constant throughout early development (Fig. 2A). *Xotch* also appeared to be expressed almost uniformly in early embryos. *Xotch* RNA was present in all three prospective germ layers isolated from late blastula embryos (Fig. 2B). Only dorsal mesoderm contained slightly more (1.5-fold) *Xotch* RNA relative to other tissues in the late blastula (16).

At later stages of development, we found that *Xotch* expression was more localized and enriched in regions where proliferation and cell determination occur, particularly in the developing nervous system. Brains and eyes isolated from newly hatched tadpoles (stage 35/36) (17) have more *Xotch* RNA than the surrounding tissues, which include both ectodermal and mesodermal derivatives (Fig. 2C). This increase may reflect the status of differentiation of these tissues at this stage, in which nonneural tissues have already begun their terminal differentiation, whereas many cells within the developing brain are still undergoing determination. This pattern of *Xotch* expression was also evident by in situ hybridization, where *Xotch* RNA was found to be localized to the developing neural tube of a stage 35/36 embryo (Fig. 3).

In the *Drosophila* eye-antennal imaginal disc, *Notch* is required for the correct differentiation of the various cell types within an ommatidium, and expression is concentrated around the morphogenetic furrow where

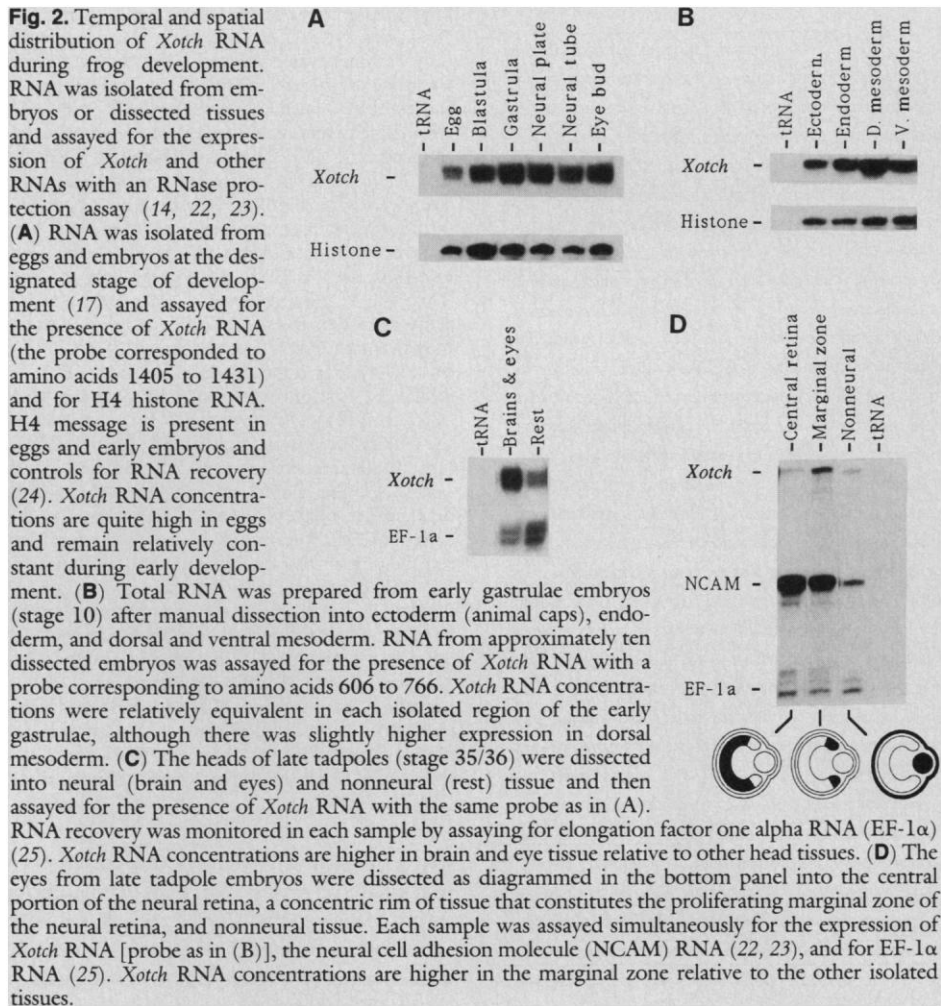


Fig. 2. Temporal and spatial distribution of *Xotch* RNA during frog development. RNA was isolated from embryos or dissected tissues and assayed for the expression of *Xotch* and other RNAs with an RNase protection assay (14, 22, 23). (A) RNA was isolated from eggs and embryos at the designated stage of development (17) and assayed for the presence of *Xotch* RNA (the probe corresponded to amino acids 1405 to 1431) and for H4 histone RNA. H4 message is present in eggs and early embryos and controls for RNA recovery (24). *Xotch* RNA concentrations are quite high in eggs and remain relatively constant during early development. (B) Total RNA was prepared from early gastrulae embryos (stage 10) after manual dissection into ectoderm (animal caps), endoderm, and dorsal and ventral mesoderm. RNA from approximately ten dissected embryos was assayed for the presence of *Xotch* RNA with a probe corresponding to amino acids 606 to 766. *Xotch* RNA concentrations were relatively equivalent in each isolated region of the early gastrulae, although there was slightly higher expression in dorsal mesoderm. (C) The heads of late tadpoles (stage 35/36) were dissected into neural (brain and eyes) and nonneural (rest) tissue and then assayed for the presence of *Xotch* RNA with the same probe as in (A). RNA recovery was monitored in each sample by assaying for elongation factor one alpha RNA (EF-1 α) (25). *Xotch* RNA concentrations are higher in brain and eye tissue relative to other head tissues. (D) The eyes from late tadpole embryos were dissected as diagrammed in the bottom panel into the central portion of the neural retina, a concentric rim of tissue that constitutes the proliferating marginal zone of the neural retina, and nonneural tissue. Each sample was assayed simultaneously for the expression of *Xotch* RNA [probe as in (B)], the neural cell adhesion molecule (NCAM) RNA (22, 23), and for EF-1 α RNA (25). *Xotch* RNA concentrations are higher in the marginal zone relative to the other isolated tissues.

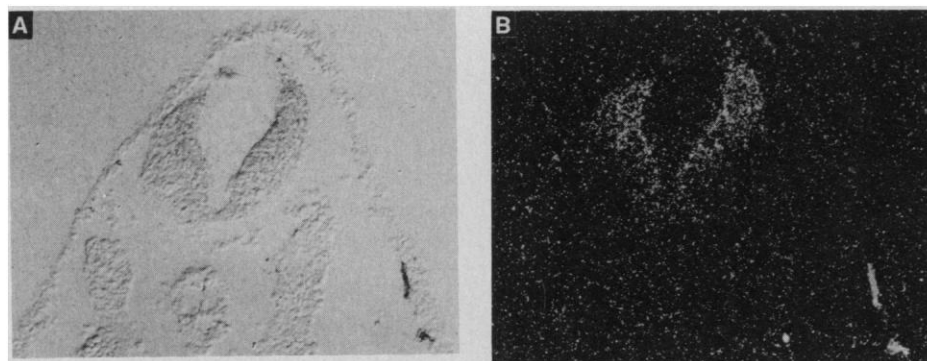


Fig. 3. In situ localization of *Xotch* RNA in a stage 35 embryo. A ^{35}S -labeled RNA probe corresponding to the COOH-terminal region of the *Xotch* protein was hybridized to tissue sections with standard techniques (22, 24) and detected by autoradiography. (A) Cross-sectional view at the level of the hindbrain photographed under Nomarski optics. (B) Same section as (A) photographed under dark-field optics to reveal autoradiography grains. The hybridization signal is concentrated in the neural tube, while surrounding mesoderm and epidermal tissues do not show hybridization above background.

cell fate is determined (15, 18). In *Xenopus*, the eye continues to grow throughout life: the central retina consists of differentiated cells and new cells are added to the periphery from pluripotent, dividing cells at the ciliary margin (19). To see if *Xotch*, like *Notch*, is expressed in regions of cell differen-

tiation in the nervous system, we dissected the peripheral and central retina from pre-metamorphic tadpoles (stage 50) and assayed for *Xotch* transcripts. *Xotch* is preferentially expressed in the marginal zone (Fig. 2D) (16). This three- to fourfold increase over central retina or nonneural eye tissues

occurs where cells are pluripotent, undergoing proliferation, and presumably interacting with other cells to achieve their determined states.

In summary, the structure of *Xotch* and its pattern of expression are similar to those observed for *Drosophila Notch*. We believe that *Xotch* and *Notch* may have equivalent functions and, therefore, that some of the basic molecular components used for cell-cell interactions and the determination of cell fate may be conserved between vertebrates and invertebrates.

REFERENCES AND NOTES

1. D. Poulson, *Proc. Natl. Acad. Sci. U.S.A.* **23**, 133 (1937); S. Artavanis-Tsakonis, *Trends Neurosci.* **4**, 95 (1988); J. A. Campos-Ortega, *ibid.* **11**, 400 (1988); U. Banerjee and S. Zipursky, *Neuron* **4**, 177 (1990).
2. S. Artavanis-Tsakonas, M. Muskavitch, B. Yedvobnick, *Proc. Natl. Acad. Sci. U.S.A.* **80**, 1977 (1983); S. Kidd, M. Kelley, M. Young, *Mol. Cell. Biol.* **6**, 3094 (1986); K. Wharton, K. Johansen, T. Xu, S. Artavanis-Tsakonas, *Cell* **43**, 567 (1985).
3. H. Vassin, K. A. Bremer, E. Knust, J. A. Campos-Ortega, *EMBO J.* **6**, 3431 (1987).
4. Complementary DNA clones encoding *Xotch* were isolated from a *Xenopus* early neurulae λ gt10 cDNA library (22). A 5.6-kb cDNA (X-1) was initially isolated by screening the library under conditions of low stringency where hybridization conditions consisted of 15% formamide, 10 mM EDTA, 200 mM NaH₂PO₄, pH 7.0, 7% SDS, and 1% bovine serum albumin (BSA) at 37°C with the EGF-like repeat regions of *Notch* and *Delta* DNA as probes (2, 3). Wash conditions consisted of 0.5 \times SSPE (26) and 0.5% SDS at 50°C. Since the 5.6-kb cDNA contained an open reading frame encoding the last two-thirds of the *Xotch* sequence, a 5' terminal restriction fragment was used to rescreen the library under high stringency to obtain the missing 5' sequences. This screen yielded a 5.0-kb cDNA clone (X-2) that overlaps with the first clone by 1 kb, extends further 5' for another 4.0 kb, and probably arose during library construction by internal priming of first strand synthesis. Both strands of the two cDNAs were sequenced with the dideoxy chain termination method as modified by the manufacturer (Sequenase, U.S. Biochemicals). The two cDNAs could be spliced together in the region of overlap to generate a composite cDNA consisting of 9324 nucleotides including a polyadenosine tract. Although it is possible that the two cDNAs are actually derived from different transcripts, it is likely that the two cDNAs represent a single transcript because the nucleotide sequence of both clones within the 1 kb of overlap is identical and Northern analysis of early embryo RNA reveals a single RNA transcript with a size of approximately 10 kb. The composite cDNA encodes a large open reading frame that begins at nucleotide 331 and terminates at nucleotide 7910. A methionine at nucleotide 343 was chosen as the site of initiation to produce the polypeptide shown in Fig. 1A.
5. I. Greenwald, *Cell* **43**, 583 (1985).
6. J. Yochem, K. Weston, I. Greenwald, *Nature* **335**, 547 (1988).
7. J. Yochem and I. Greenwald, *Cell* **58**, 553 (1989); J. Austin and J. Kimble, *ibid.*, p. 565.
8. L. Breeden and K. Nasmyth, *Nature* **329**, 651 (1987); B. Andrews and I. Herskowitz, *ibid.* **342**, 830 (1989); S. Lux, K. John, V. Bennette, *ibid.* **344**, 36 (1990); A. Spence, A. Coulson, J. Hodgkin, *Cell* **60**, 981 (1990); H. Ohno, G. Takimoto, T. McKeithan, *ibid.*, p. 991.
9. D. Hartley, T. Xu, S. Artavanis-Tsakonas, *EMBO J.* **6**, 3407 (1987).
10. M. Kelley, S. Kidd, W. Deutsch, M. Young, *Cell* **51**, 539 (1987).
11. K. Wharton, B. Yedvobnick, V. Finnerty, S. Artavanis-Tsakonas, *ibid.* **40**, 55 (1985); W. McGinnis,

- R. L. Garber, J. Wirz, A. Kuroiwa, W. Gehring, *ibid.* 37, 403 (1984).
12. A. Kishimoto *et al.*, *J. Biol. Chem.* 260, 12492 (1985); J. R. Woodgett, K. L. Gould, T. Hunter, *Eur. J. Biochem.* 161, 177 (1986); P. R. Vulliet, F. L. Hall, J. P. Mitchell, D. G. Hardie, *J. Biol. Chem.* 264, 16292 (1989).
 13. M. Rechsteiner, in *Advances in Enzyme Regulation*, G. Weber, Ed. (Pergamon, New York, 1988), vol. 27, pp. 135–151; S. Rogers, R. Wells, M. Rechsteiner, *Science* 234, 364 (1986).
 14. D. A. Melton *et al.*, *Nucleic Acids Res.* 12, 7035 (1984).
 15. K. Johansen, R. Fehon, S. Artavanis-Tsakonas, *J. Cell Biol.* 109, 2427 (1989); S. Kidd, M. Baylies, G. Gasic, M. Young, *Genes Dev.* 3, 1113 (1989).
 16. Quantitative analysis was performed with a laser densitometer (Pharmacia LKB) and AMBIS software (San Diego). Exposures were chosen that were within the linear response range of the film and the values were normalized to the control RNAs.
 17. P. D. Nieuwkoop and J. Faber, *Normal Table of Xenopus laevis* (North-Holland, Amsterdam, 1967).
 18. R. Cagan and D. Ready, *Genes Dev.* 3, 1099 (1989).
 19. J. G. Holleyfield, *Dev. Biol.* 18, 163 (1968).
 20. Nucleotide and amino acid sequence information is available through GenBank accession number M33874.
 21. J. Devereux, P. Haeblerli, O. Smithies, *Nucleic Acids Res.* 12, 387 (1984).
 22. C. R. Kintner and D. A. Melton, *Development* 99, 311 (1987).
 23. J. Dixon and C. Kintner, *ibid.* 106, 749 (1989).
 24. D. A. Melton, *Nature* 328, 80 (1987).
 25. P. Krieg, S. Varnum, W. Wormington, D. A. Melton, *Dev. Biol.* 133, 93 (1989).
 26. T. Maniatis, E. Fritsch, J. Sambrook, *Molecular Cloning: A Laboratory Manual* (Cold Spring Harbor Laboratory, Cold Spring Harbor, NY, 1982), p. 447.
 27. We thank S. Artavanis-Tsakonas, J. Campos-Ortega, and E. Knust for providing the *Drosophila Notch* and *Delta* DNAs, A. Newman for technical assistance, D. Ades for the densitometry scans, and C. Holt, G. Lemke, and J. Thomas for critical reading of the manuscript. We gratefully acknowledge support from the NIH and March of Dimes. C.K. is a research fellow of the McKnight and Sloan Foundations.

12 April 1990; accepted 18 June 1990

Calmodulin Activation of Calcium-Dependent Sodium Channels in Excised Membrane Patches of *Paramecium*

Y. SAIMI* AND K.-Y. LING

Calmodulin is a calcium-binding protein that participates in the transduction of calcium signals. The electric phenotypes of calmodulin mutants of *Paramecium* have suggested that the protein may regulate some calcium-dependent ion channels. Calcium-dependent sodium single channels in excised patches of the plasma membrane from *Paramecium* were identified, and their activity was shown to decrease after brief exposure to submicromolar concentrations of calcium. Channel activity was restored to these inactivated patches by adding calmodulin that was isolated from *Paramecium* to the cytoplasmic surface. This restoration of channel activity did not require adenosine triphosphate and therefore, probably resulted from direct binding of calmodulin, either to the sodium channel itself or to a channel regulator that was associated with the patch membrane.

CALMODULIN (CAM) PARTICIPATES in signal transduction processes in most cells. In particular, CaM regulates the activation of certain calcium (Ca^{2+})-dependent potassium (K^+) channels (1, 2), the inhibition of the Ca^{2+} -release channel activity of the sarcoplasmic reticulum (3), and, perhaps, the gap junction channel (4). However, the mechanism by which CaM regulates ion channel activity is not well understood. CaM may interact directly with channel proteins, as suggested in cell-free systems (2, 3) or may affect channel activity through Ca^{2+} , CaM-dependent covalent modifications of the channel proteins (5). In addition, CaM may control transcription of genes, as suggested in plants (6), possibly including those that encode ion

channels.

CaM regulates ion channels in *Paramecium*. Mutations in the CaM structural gene eliminate one or more of three Ca^{2+} -dependent ion currents recorded under whole-cell voltage clamp (7). To decipher the mechanism of CaM regulation of ion channels in *Paramecium*, we used a patch-clamp technique to study Ca^{2+} -dependent sodium (Na^+) single channels in excised patches from *Paramecium*.

Previous studies with whole-cell *Paramecium* have shown that activation of the Na^+ conductance is dependent on cytoplasmic, free Ca^{2+} , and that the Na^+ channel is permeable to Na^+ and lithium (Li^+), but not potassium (K^+) or cesium (Cs^+) (8); similar conductances have been found in other organisms (9). With 100 mM Na^+ in both pipette and bath (10), patch-clamp recordings (11) revealed single-channel activities (Fig. 1A) in excised inside-out patches of the plasma membrane from *P. tetraure-*

lia (12) when 10^{-5} M free Ca^{2+} was present in the bath (on the cytoplasmic side of the patch). The channel was more active at positive than at negative voltages. The current amplitude, measured from the amplitude histograms, was plotted as a function of membrane voltage (I-V plot), and the conductance was determined to be 19.0 pS [± 3.2 (mean \pm standard deviation, SD), $n = 10$; error limits of \pm SD are used throughout the report] (Fig. 1B) (13).

The ion selectivity of the channel (14) was determined by substitution of Na^+ in the bath with other ions. From I-V plots of single-channel currents under bi-ionic conditions (Fig. 1C) and reversal potential analyses (15) (Fig. 1D), we determined the relative permeability ratios of $\text{Na}^+:\text{Li}^+:\text{K}^+:\text{Cs}^+$ to be 1:0.76:0.07:0.05, respectively ($n = 3$). The conductance and ion selectivity of the Na^+ single channel in *Paramecium* were therefore similar to those of its counterparts in higher organisms, which are voltage- and not Ca^{2+} -gated (16).

The Ca^{2+} dependence of the *Paramecium* Na^+ channel was examined by changing the free Ca^{2+} concentration of the bath. After measuring the channel activity at 10^{-5} M Ca^{2+} (Fig. 2A, left), the bath was perfused with a solution of 10^{-8} M Ca^{2+} , and the channel activity at all voltages fell nearly to zero (Fig. 2A, middle). This suggested that the channel activity was Ca^{2+} dependent. However, a return to 10^{-5} M Ca^{2+} after brief exposure to 10^{-8} M Ca^{2+} failed to restore channel activity (Fig. 2A, right). The initial activity at 10^{-5} M Ca^{2+} was reduced upon returning to 10^{-5} M Ca^{2+} after exposure to 10^{-8} M Ca^{2+} for 60 s [1.19 ± 1.04 versus 0.08 ± 0.12 , expressed as the activity of all channels in the patch (NPo) at -50 mV, $n = 6$; 60 to 150 s elapsed between the two measurements] (17). By contrast, continuous exposure to 10^{-5} M Ca^{2+} for similar durations (Fig. 2B) did not alter channel activity, which varied from 1.20 ± 0.59 to 1.26 ± 0.88 ($n = 8$, 55 to 175 s elapsed, including a 30- to 140-s perfusion period). However, even at 10^{-5} M Ca^{2+} , the channel activity declined with prolonged exposure (>30 min). These findings suggested that a factor or factors required for Na^+ -channel activity was rapidly degraded or inactivated by exposure to 10^{-8} M Ca^{2+} .

Because the Ca^{2+} -dependent Na^+ conductance of *Paramecium* is under the control of calmodulin (CaM) in vivo (7), we tested whether CaM, when applied to the cytoplasmic surface of the patch membrane, could restore activity to inactivated Na^+ channels in vitro. When channel activity had declined, we added *Paramecium* CaM (2 μg , $>85\%$ pure) (18) to the 300- μl bath that contained 10^{-5} M Ca^{2+} . We observed an increase in

Laboratory of Molecular Biology, University of Wisconsin-Madison, Madison, WI 53706.

*To whom correspondence should be addressed.